Sensors and Materials, Vol. 34, No. 11 (2022) 4053–4069
MYU Tokyo

S & M 3096

Terrestrial Water Storage Changes over the Last 20 Years in the Amazon Basin

Kuifeng Luan,[1,2] Jiancong Hu,[1] Guiping Feng,[1,2*] Zhenge Qiu,[1,2]
Kunning Zhang,[1] Weidong Zhu,[1,2] Jie Wang,[1] and Zhenhua Wang[3]

[1]College of Marine Sciences, Shanghai Ocean University, Shanghai 201306, China
[2]Shanghai Engineering Research Center of Estuarine and Oceanographic Mapping, Shanghai 201306, China
[3]College of Information Technology, Shanghai Ocean University, Shanghai 201306, China

(Received August 5, 2022; accepted October 20, 2022)

Keywords: terrestrial water storage changes, GRACE-FO, Amazon Basin, precipitation, surface temperature

The Amazon Basin is the world's largest flowing basin and plays an important role in the global hydrological cycle. We combined 20 years of Gravity Recovery and Climate Experiment (GRACE), Swarm, and GRACE Follow-On (GRACE-FO) satellite data to investigate variations of the terrestrial water storage (TWS) from April 2002 to December 2021. We also analyzed the effects of precipitation, surface temperature, and evapotranspiration on TWS changes. Compared with different methods of processing GRACE data, we found that the combined filtering method of P4M6 + Gaussian 300 km in GRACE/GRACE-FO data provided the most accurate results. The long-term trend of TWS was an increase of approximately 0.23 ± 0.11 cm/a in the Amazon Basin, and the central and eastern regions had the highest increase rate, whereas the southeastern region showed a decreasing trend. In the last 20 years, maximum TWS variations occurred in April and minimum TWS variations occurred in October. In spring, the TWS in the Amazon Basin changes considerably from north to south (increasing in the north and decreasing in the south), opposite to that in winter. In the Amazon Basin, precipitation and surface temperature are the important factors affecting the TWS changes, unlike evapotranspiration. In October 2020, the anomalous decreases in TWS changes correlate with insufficient precipitation and rising surface temperatures, which results in a drought.

1. Introduction

Terrestrial water storage (TWS), which includes groundwater, snow and ice, soil moisture and permafrost, surface water, and wet biomass (canopy), plays a key role in water resource management and land–surface processes in the climate system, such as predicting potential flood hazards and understanding land–atmosphere energy balance and exchange. Traditional methods of monitoring TWS rely on weather stations, tide gauge stations, wells, and other carriers. Accuracy is limited owing to varying equipment and observation conditions, which is

*Corresponding author: e-mail: gpfeng@shou.edu.cn
https://doi.org/10.18494/SAM4073

ISSN 0914-4935

not conducive to reliable long-term data acquisition. The recent launch of a series of gravity satellites has solved this problem, which can make continuous, rapid, and repeated observations, and such gravity satellites have become widely used in the field of TWS monitoring.

Gravity Recovery and Climate Experiment (GRACE) is a twin satellite mission jointly sponsored by the National Aeronautics and Space Administration (NASA) and German Aerospace Center (DLR). The two identical satellites orbit behind each other in the same orbital plane at an approximate distance of 220 km. GRACE uses a K-band ranging system to provide precise measurements of the distance change between the two satellites. Each satellite carries a Global Positioning System (GPS) receiver of geodetic quality and high-accuracy accelerometers to enable accurate orbit determination, the spatial registration of gravity data, and the estimation of gravity field models. Since its launch in March 2002, GRACE has provided global measurements of gravity change with unprecedented accuracy at approximately monthly intervals. GRACE has also provided a unique opportunity to monitor TWS changes in the Amazon Basin, including interannual and long-term changes (see, for example, Refs. 1–8), but the GRACE mission ended in June 2017.

To continue the data acquisition, GRACE Follow-On (GRACE-FO) was launched in May 2018 and has continued to monitor global gravity field variations. The two GRACE-FO satellites use the same type of microwave ranging system as GRACE. However, GRACE-FO also carries something new: a laser ranging interferometer (LRI). GRACE-FO's interferometer detects changes at a distance more than 10 times smaller than what a microwave instrument detects. However, there is a gap of almost one year between the end of the GRACE mission and the successful launch of GRACE-FO, and studies on TWS changes in the Amazon Basin during this gap are few. Lück *et al.* used GRACE and Swarm data to invert the Amazon Basin mass changes, and found that the Swarm results are similar to the GRACE results, but with more pronounced noise.[9] Cui *et al.* combined GRACE, GRACE-FO, and Swarm satellite data to calculate the TWS changes, and found that the linear trend was −0.72 cm/a in the Amazon Basin from December 2013 to May 2020.[10] Xiang *et al.* combined GRACE, GRACE-FO, Swarm, and Global Land Data Assimilation System (GLDAS) data to invert the TWS changes in the Amazon Basin from 2010 to 2020, and found that the drought may intensify after 2015.[11] Li *et al.* used Swarm and GRACE data to estimate TWS changes in the Amazon Basin during the 2015–2016 drought, and demonstrated the potential of Swarm to replace GRACE in detecting extreme drought and flood disasters.[12]

With the successful launch of the GRACE-FO satellites, observations of monthly gravity fields have been accumulated for nearly 20 years. However, the analysis of factors affecting TWS changes in the Amazon Basin is still insufficient at present. To ensure the temporal continuity of TWS observations and study the latest TWS changes in the Amazon Basin, we used the Swarm data to fill the gap between GRACE and GRACE-FO data. We combined GRACE, Swarm, and GRACE-FO satellite data to estimate the TWS changes in the Amazon Basin over the last 20 years (April 2002–December 2021) and compared the results with the GLDAS model. We analyzed the spatial and temporal characteristics of the TWS changes and used the Global Precipitation Climatology Project (GPCP) precipitation data, Climatic Research Unit Time series (CRU TS) temperature data, and GLDAS evapotranspiration data to further

analyze the factors affecting the TWS changes. We also explored the reasons for the 2009 flood and 2020 drought disasters in the Amazon Basin.

2. Observation Data and Processing Methods

2.1 Observation data

The Amazon Basin is located in the central and eastern regions of South America. It is the world's largest basin (in terms of flow and area), with a total area of approximately 7.05×10^6 km^2, which is approximately 40% of the total area of South America.[4] The Amazon Basin is east of the Andes Mountains, extending from the Guyana Plateau in the north to the Brazilian Plateau in the south, with high topography in the west, an average elevation of approximately 4000 m, and low topography in the east.[13] The Amazon Basin is a complex ecosystem containing the largest tropical rainforest area in the world and plays an important role in the global hydrological cycle and global climate change.[14]

The GRACE/GRACE-FO data was provided by the Center for Space Research (CSR), University of Texas, Austin. In this paper, we used the GRACE RL06 data from April 2002 to June 2017 and the GRACE-FO RL06 data from June 2018 to December 2021, and missed 22 months (namely, June 2002, July 2002, June 2003, January 2011, June 2011, May 2012, October 2012, March 2013, August 2013, September 2013, February 2014, July 2014, December 2014, June 2015, October 2015, November 2015, April 2016, September 2016, October 2016, February 2017, August 2018, and September 2018). Over the 204-month period, we calculated the average spherical harmonic coefficient and then subtracted the average from the monthly data to obtain the gravity field anomalies. The coefficients of monthly gravity field were truncated to the degree and order of 60. Tidal and non-tidal atmospheric and high-frequency ocean signals were removed.[15]

Swarm data were provided by the Astronomical Institute at the Czech Academy of Sciences (ASU). The data were truncated to the degree and order of 40, and covered the period of December 2013 to December 2021. Teixeira *et al.* reported that the accuracy of the geodetic level error was consistent with GRACE when the coefficients of Swarm time-variable gravity field were below the degree and order of 10.[16] Therefore, we used the first 10 orders of the Swarm time-variable gravity field models to calculate the TWS changes in the Amazon Basin.

The GLDAS model has been jointly developed by the National Aeronautics and Space Administration/Goddard Space Flight Center (NASA/GSFC) and the National Oceanic and Atmospheric Administration/National Centers for Environmental Prediction (NOAA/NCEP). It is a global, high-resolution terrestrial modeling system incorporating ground and satellite observations in order to provide optimal simulations of global land surface states and fluxes in near real time. The land water storage in the GLDAS model includes soil moisture, snow, and canopy water. In this paper, we used the NOAH land surface model with $1° \times 1°$ resolution from January 2002 to December 2021. To compare with GRACE, Swarm, and GRACE-FO results, the same Gaussian filter and de-striping filter were used to eliminate the error of the GLDAS model.

To investigate the effect of precipitation on the TWS changes in the Amazon Basin, we used precipitation data from the GPCP. The data is based on infrared and microwave satellite data and surface rain gauge observations. The GPCP provides global monthly average precipitation data, and we used GPCP monthly precipitation data in a 2.5° × 2.5° latitude-longitude grid from April 2002 to December 2021.

To investigate the effect of surface temperature on the TWS changes in the Amazon Basin, we used surface temperature data from the CRU TS. The CRU TS data was developed by the UK's National Centre for Atmospheric Science (NCAS), including 10 climate variables such as temperature, humidity, and cloud cover for the global land surface. We used the monthly surface temperature data of CRU TS with a spatial resolution of 0.5° × 0.5° from April 2002 to December 2020. The self-calibrating Palmer Drought Severity Index (scPDSI) data is also derived from the CRU TS, which is a drought index that describes the severity of drought. We used the monthly scPDSI data of CRU TS with a spatial resolution of 0.5° × 0.5° from April 2002 to December 2020.

2.2 Processing methods

TWS changes can be directly estimated on the basis of gravity coefficient anomalies for each month. We used the equivalent water height (EWH) $\Delta h_w(\theta, \lambda)$ to express the TWS[17]:

$$\Delta h_w(\theta,\lambda) = \frac{R\rho_e}{3}\sum_{l=0}^{\infty}\sum_{m=0}^{l}\frac{2l+1}{1+k_l}\left[\Delta C_{lm}\cos(m\lambda)+\Delta S_{lm}\sin(m\lambda)\right]\dot{P}_{lm}(\cos\theta), \quad (1)$$

where θ is the geocentric residual latitude, λ is the geocentric longitude, R is the radius of Earth at the equator, ρ_e is the average density of Earth, l and m are the degree and order of the gravity field, respectively, k_l is the loading love number, ΔC_{lm} and ΔS_{lm} are the variations in the Stokes coefficients, and $\dot{P}_{lm}$ is the normalized Legendre function.

We have to make a series of corrections to obtain the precise TWS changes. First, the 300 km width of the Gaussian filter was used to reduce the errors at high degrees.[18] Then, monthly degree 1 coefficients from Swenson *et al.* were used.[19] Since GRACE is not sensitive to the degree 2 and order 0 (C_{20}) coefficients, the C_{20} coefficients were replaced by Satellite Laser Ranging (SLR) solutions.[20] The ICE-5G model was used to eliminate the effects of the glacial isostatic adjustment on the estimation results.[21] Although Gaussian filtering can reduce the high-order spherical harmonic coefficient noise, it cannot eliminate the effect of the systematic correlation error. Swenson and Wahr proposed the polynomial fit method to eliminate the systematic correlation error, called Swenson filtering.[22] Duan *et al.* proposed a refined approach for choosing parameters of decorrelation filtering, called Duan filtering.[23] Chen *et al.*[24] and Chambers and Bonin[25] proposed the PnMl decorrelation filtering method.

We calculated the TWS changes in the Amazon Basin over the most recent 20 years and analyzed the effects of different filtering methods. The results are shown in Table 1. The root mean square error (RMSE) obtained using a P4M6 + Gauss 300 km combined filtering method was 6.81 cm, which was the smallest RMSE among the four combined filtering methods. The

Table 1
Statistical results of TWS changes obtained with different filtering methods.

Model and filtering method	Max (cm)	Min (cm)	RMSE (cm)
GLDAS	10.66	−13.02	—
Swenson + Gauss 300 km	22.76	−20.86	7.02
Duan + Gauss 300 km	23.14	−22.31	7.46
P4M6 + Gauss 300 km	23.04	−20.48	6.81
P4M15 + Gauss 300 km	22.79	−20.98	6.96

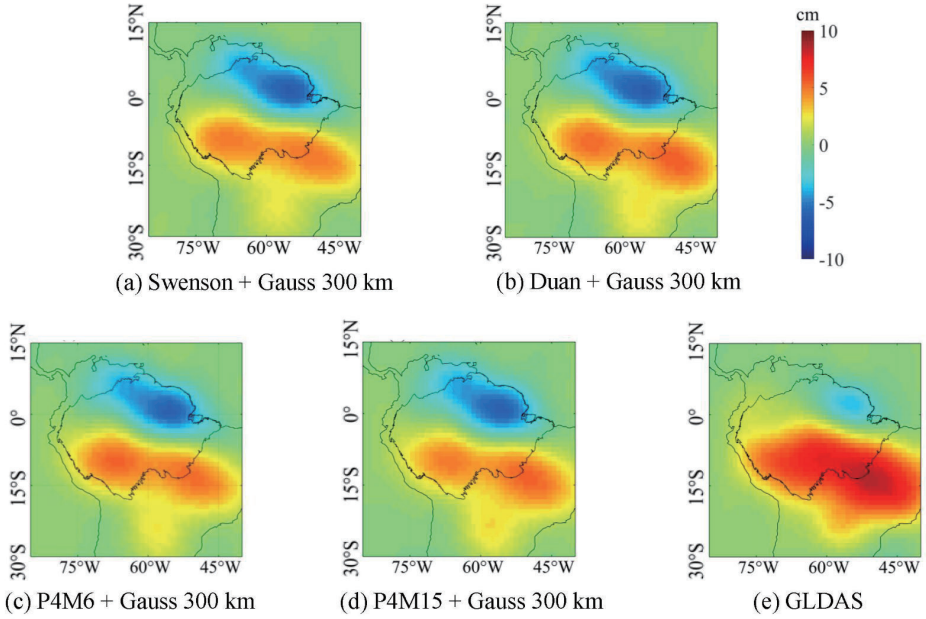

Fig. 1. (Color online) TWS changes (in cm of equivalent water height) in the Amazon Basin in autumn 2006.

TWS changes in autumn 2006 with different methods of processing GRACE data are shown in Fig. 1. As shown in Fig. 1, the results obtained using the P4M6 + Gauss 300 km combined filtering method were the most consistent with the GLDAS results. Therefore, the P4M6 + Gauss 300 km combined filter was used to process the GRACE/GRACE-FO data in subsequent analyses.

To analyze the effects of precipitation, surface temperature, and evapotranspiration on TWS changes, we used Pearson correlation coefficients to describe the correlation between the two variables x and y. The Pearson correlation coefficient r is calculated using the formulas shown below. A strong correlation means that the absolute value of the correlation coefficient is greater than 0.6, a weak correlation means that the absolute value of the correlation coefficient is less than 0.4, and a moderate correlation means that the absolute value of the correlation coefficient is between 0.4 and 0.6.

$$r = \frac{\sum_{i=1}^{n}(x_i - \bar{x})(y_i - \bar{y})}{\sqrt{\sum_{i=1}^{n}(x_i - \bar{x})^2 \sum_{i=1}^{n}(y_i - \bar{y})^2}} \tag{2}$$

$$\bar{x} = \frac{1}{n}\sum_{i=1}^{n} x_i, \bar{y} = \frac{1}{n}\sum_{i=1}^{n} y_i \tag{3}$$

3. Results and Discussion

3.1 Secular variations of TWS

We used the GRACE (April 2002 to June 2017), Swarm (July 2017 to May 2018), and GRACE-FO (June 2018 to December 2021) data to calculate the time series of the TWS changes in the Amazon Basin over the last 20 years, as shown in Fig. 2. In general, the GRACE, Swarm, and GRACE-FO results agreed well with the GLDAS results. Conversely, the GRACE/GRACE-FO results had more prominent amplitudes than the GLDAS results. This is mainly because the GLDAS model underestimates data such as groundwater.[26] The GRACE, Swarm, and GRACE-FO results revealed that the TWS changes in the Amazon Basin over the last 20 years (April 2002 to December 2021) had an increasing trend at a rate of approximately 0.23 ± 0.11 cm/a.

The EWHs of TWS changes in the Amazon Basin observed by GRACE were −19.99 cm in October 2005 and 23.04 cm in May 2009. These results were consistent with the extreme drought in 2005 and the extreme flood in 2009 in the Amazon Basin, respectively, which were discussed by Chen and coworkers.[3,4] As observed by GRACE, the EWHs of TWS changes in the Amazon Basin were −20.48 cm in October 2010 and 20.53 cm in March 2012, which were consistent with the drought peak in October 2010 and the flood peak in March 2012, respectively, as discussed

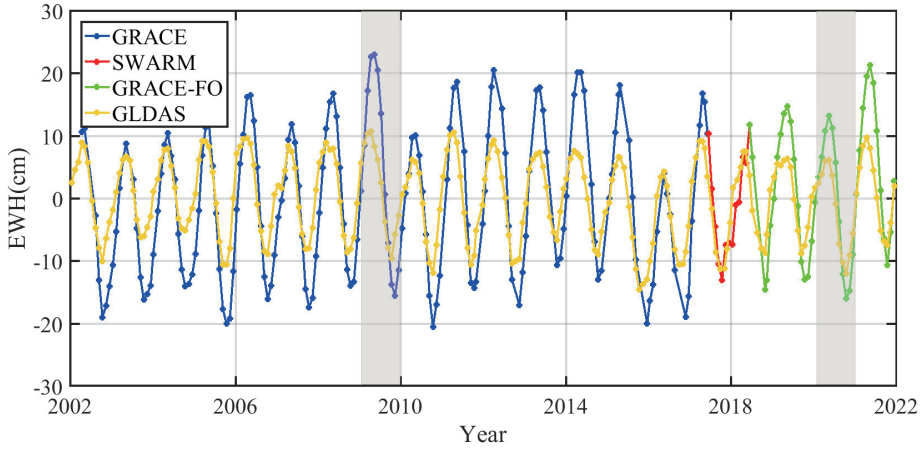

Fig. 2. (Color online) Time series of TWS changes based on GRACE, Swarm, GRACE-FO, and GLDAS results in the Amazon Basin over the last 20 years.

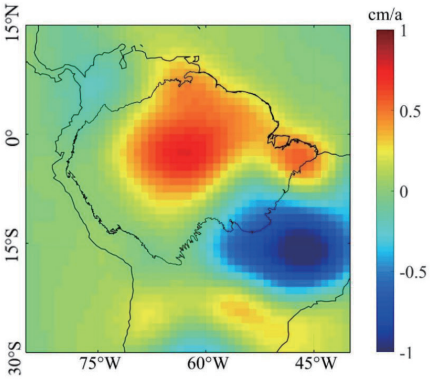

Fig. 3. (Color online) Long-term trend of TWS changes in the Amazon Basin over the last 20 years.

by Nie *et al.*[6] The EWH of TWS changes was −19.95 cm in October 2016, which was consistent with the extreme drought in 2016 in the Amazon Basin.[27]

Further analysis of the spatial variation characteristics of TWS changes in the Amazon Basin over the last 20 years is shown in Fig. 3. The TWS changes in the Amazon Basin had an overall increasing trend with obvious spatial distribution heterogeneity. Locally, the rate of the TWS changes in the western region of the Amazon Basin was close to zero, with no obvious changes in relatively stable water storage. The TWS changes increased with a maximum rate of 0.76 cm/a in the central and eastern regions and decreased with a minimum rate of −0.84 cm/a in the southeastern region. The southeastern region is located in the northern section of Brazil, and the decrease may be due to the overextraction of groundwater by humans in agriculture and related irrigation activities.[28]

3.2 Seasonal variations of TWS

To further investigate the seasonal variations of TWS, we used the least square method to fit the time series of TWS changes in the Amazon Basin over the last 20 years. The results are shown in Table 2. The GRACE/GRACE-FO results show that the annual phase is approximately 123°, indicating that the maximum TWS changes in the Amazon Basin occur at the end of April, whereas the GLDAS model results suggest that the maximum TWS changes occur in the middle of April. There is a phase difference of approximately 17 days between the two results. Therefore, the GRACE/GRACE-FO observations are relatively lagging. In terms of semiannual amplitudes, the GLDAS model results agreed well with the GRACE/GRACE-FO results.

Figure 4 shows the monthly average TWS changes in the Amazon Basin over the last 20 years. The difference between the GRACE-FO results and the GLDAS model results is large in January, April–July, and October–December, with the variation exceeding 5 cm. The largest variation was observed in November (reaching 8.46 cm), which is mainly due to the underestimation of GLDAS subsurface water.

We further analyzed the seasonal spatial patterns of TWS changes in the Amazon Basin by using 2006 as an example. As shown in Fig. 5, in spring, the TWS in the Amazon Basin varies greatly from north to south, with an increase in the northern region and a decrease in the

Table 2
Annual and semiannual variations of TWS changes based on different filtering methods in the Amazon Basin from April 2002 to December 2021.

Model and filtering method	Annual		Semiannual	
	Amplitude (cm)	Phase (°)	Amplitude (cm)	Phase (°)
GLDAS	7.9	105.3	1.0	320.6
Swenson + Gauss 300 km	14.7	123.2	0.6	338.1
Duan + Gauss 300 km	16.1	123.1	0.8	332.9
P4M6 + Gauss 300 km	15.2	122.3	0.7	328.1
P5M12 + Gauss 300 km	15.4	122.7	0.7	332.7

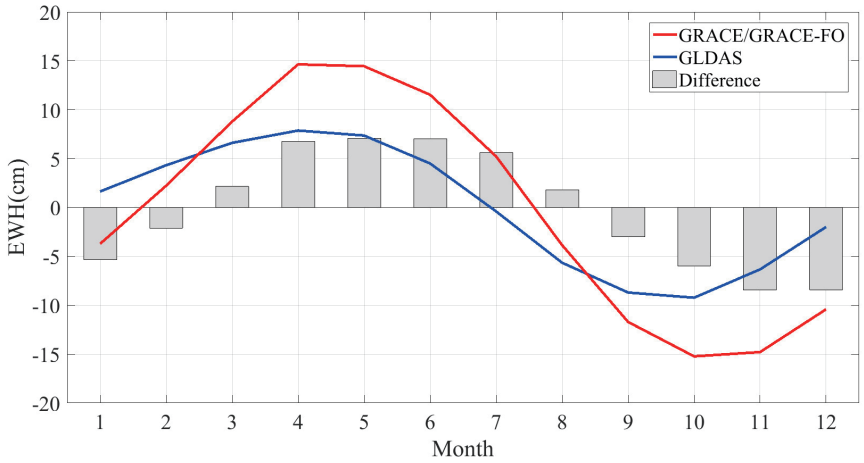

Fig. 4. (Color online) Average monthly TWS changes in the Amazon Basin from April 2002 to December 2021

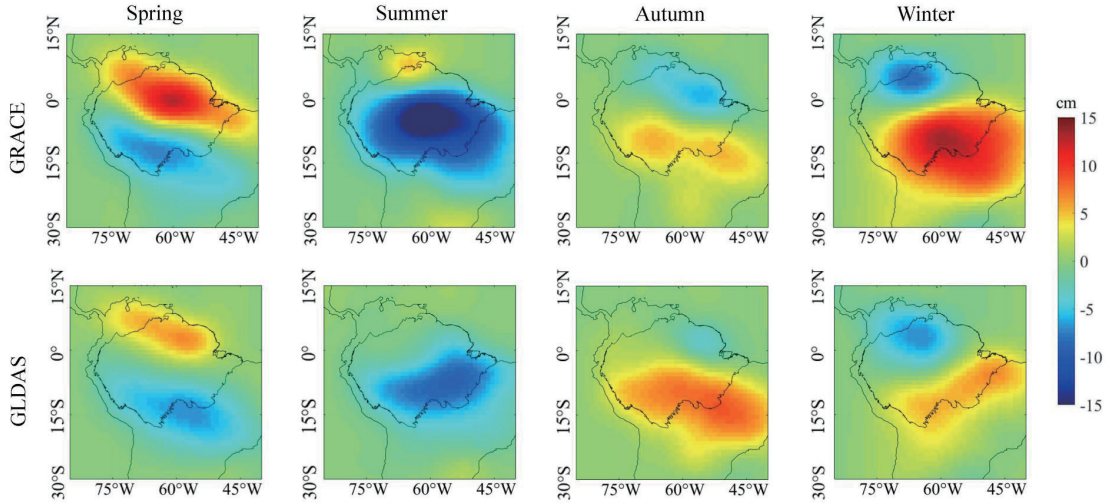

Fig. 5. (Color online) TWS changes (in cm of equivalent water height) in the Amazon Basin in four seasons of 2006.

southern region. The summer is the season with the least amount of water stored. The TWS increases in autumn when compared with summer, with characteristics of low in the northern region and high in the southern region. In winter, the TWS is the opposite to that in spring, with a decrease in the northern region and an increase in the southern region.

3.3 Effects of TWS

3.3.1 Precipitation

To study the factors affecting the TWS changes in the Amazon Basin, the monthly precipitation changes were computed by removing the average monthly estimates from January 2003 to December 2020. We analyzed the correlation between the TWS and GPCP precipitation changes in the Amazon Basin, as shown in Fig. 6. The fluctuation patterns of the TWS and GPCP precipitation changes in the Amazon Basin are relatively consistent. The TWS changes lag behind the precipitation changes by approximately 64 days and have a larger amplitude, which is mainly due to the TWS changes observed by GRACE, Swarm, and GRACE-FO including the precipitation changes before that month. The correlation coefficient between them is 0.57, which suggests a moderate correlation. However, the correlation coefficient between the precipitation changes with a lag of two months and the TWS changes is 0.85, showing a strong correlation. This result reveals that precipitation is an important factor affecting the TWS changes in the Amazon Basin.

3.3.2 Surface temperature

To investigate the effect of temperature on the TWS changes in the Amazon Basin, the monthly surface temperature changes were computed by removing the average monthly estimates from January 2003 to December 2020. As shown in Fig. 7, the TWS changes negatively correlate with surface temperature changes, with a correlation coefficient of −0.50, which suggests that they are moderately negatively correlated, indicating that surface temperature affects the TWS changes in the Amazon Basin.

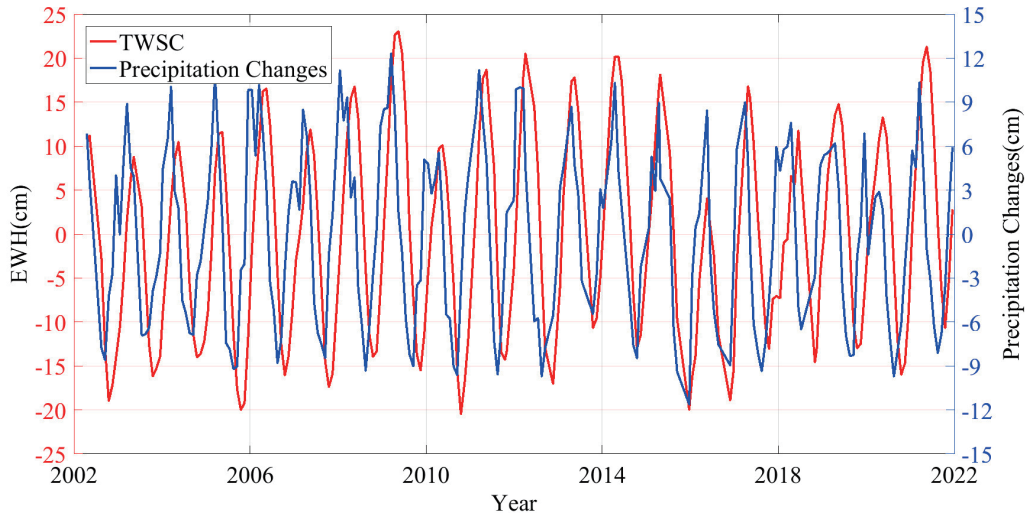

Fig. 6. (Color online) Time series of the monthly TWS and GPCP precipitation changes in the Amazon Basin.

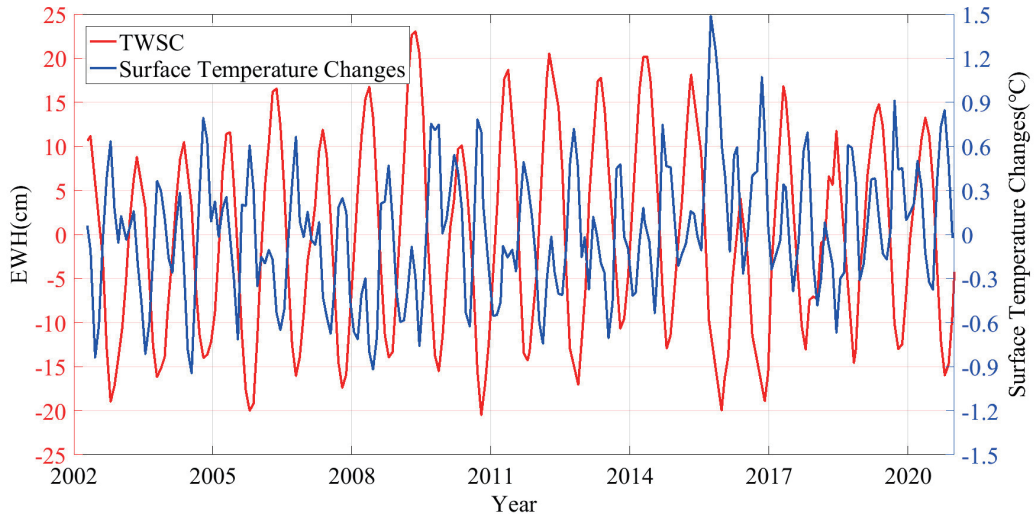

Fig. 7. (Color online) Time series of the monthly TWS and surface temperature changes in the Amazon Basin.

3.3.3 Evapotranspiration

To further understand the effect of evapotranspiration on the TWS changes in the Amazon Basin, we obtained evapotranspiration changes after removing the average monthly estimates from January 2003 to December 2020. As shown in Fig. 8, the TWS changes in the Amazon Basin positively correlate with evapotranspiration changes, with a correlation coefficient of 0.29, which is a weak correlation, indicating that the relationship between the TWS changes and evapotranspiration changes in the Amazon Basin is not significant.

3.4 Drought index

Water storage deficit (WSD) is the difference between the monthly water storage change and the average of the corresponding month. We standardized the time series of WSD data to obtain the water storage deficit index (WSDI) as follows:

$$WSD_{i,j} = TWSC_{i,j} - \overline{TWSC_j}, \tag{4}$$

$$WSDI = \frac{WSD - \mu}{\sigma}, \tag{5}$$

where $TWSC_{i,j}$ represents the TWS changes in the i year ($2002 \le i \le 2020$) j month ($1 \le j \le 12$), $\overline{TWSC_j}$ is the mean deviation of TWS changes in the j month, and μ and σ are the mean and standard deviation of the WSD, respectively. When the WSDI is negative and lasts for more than three months, drought is considered to occur during that time period. Drought duration equals the number of months between the start and end months of the drought. Peak magnitude indicates the maximum of monthly WSDI during the drought, and average magnitude indicates the monthly average of WSDI during the drought. The drought severity S is as follows:

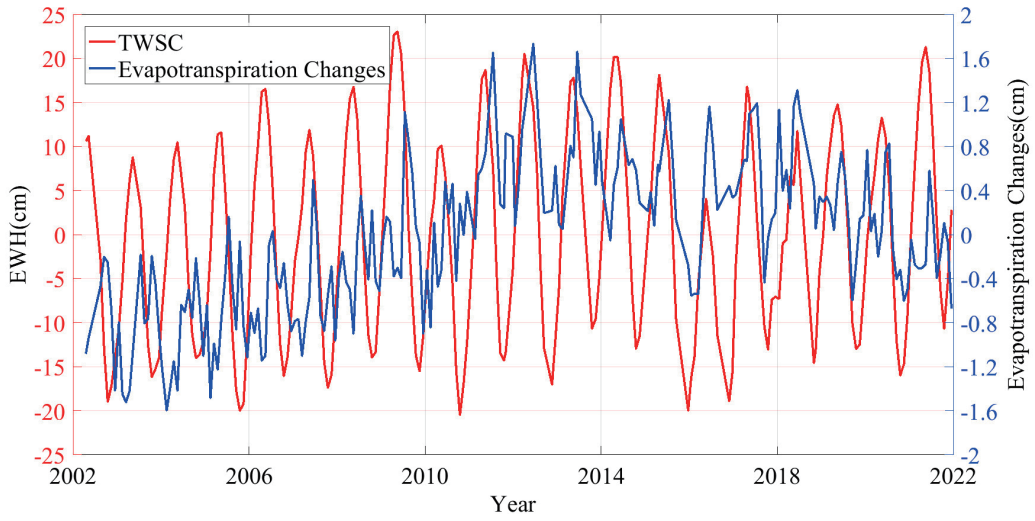

Fig. 8. (Color online) Time series of the monthly TWS and evapotranspiration changes in the Amazon Basin.

$$S = \bar{M} \times D, \tag{6}$$

where $\bar{M}$ is the average magnitude and D is the drought duration.

We calculated the time series of the monthly WSDI from April 2002 to December 2020. To verify the accuracy of the WSDI results, we compared the WSDI results with the scPDSI results. As shown in Fig. 9, there is a relatively good agreement between the WSDI and scPDSI results, with a correlation coefficient of 0.62. Therefore, it is reliable to use WSDI to detect drought events in the Amazon Basin.

Table 3 shows the drought events detected by WSDI in the Amazon Basin and the characteristics of each drought event. The Amazon Basin experienced 10 drought events from April 2002 to December 2020 on the basis of the WSDI results. The longest duration was the drought that started in November 2009 and lasted 14 months, with an average magnitude of −0.60 and a peak magnitude of −1.11. The most severe drought event occurred from December 2015 to December 2016, with a drought severity of −27.90 and an average magnitude of −2.15. The most recent drought event in the Amazon Basin occurred from March 2020 to October 2020, and the average magnitude was –0.79. In addition, there were numerous minor droughts in the Amazon Basin with low severity values or short durations. The previous studies have demonstrated the validity of our results (Table 3).

3.5 Typical flood and drought disasters in the Amazon Basin

In May 2009, TWS changes revealed a maximum of 23.04 cm in the Amazon Basin over the last 20 years. GPCP changes showed a continuous and positive rainfall pattern from December 2008 to May 2009, and reached a maximum of 12.33 cm in March 2009. The CRU showed continuous and negative surface temperature changes from December 2008 to July 2009, and reached a minimum in January 2009 (−0.60 °C). From December 2008 to May 2009, the

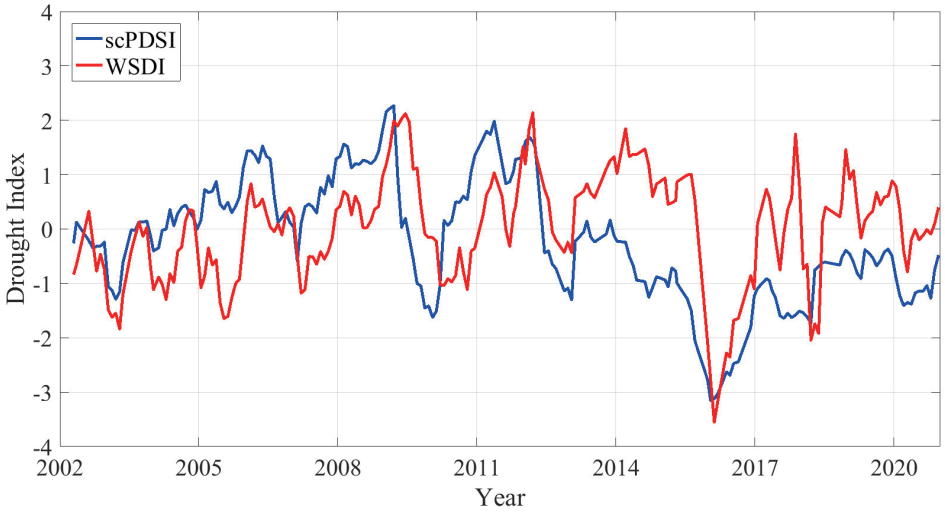

Fig. 9. (Color online) Time series of the monthly scPDSI and WSDI in the Amazon Basin.

Table 3
Summary of drought events detected by WSDI in the Amazon Basin.

Drought event	Time span	Duration (months)	Peak magnitude	Average magnitude	Drought severity	Reference
1	200209–200305	9	–1.84	–1.10	–9.89	5
2	200312–200408	9	–1.11	–0.84	–7.58	10
3	200412–200512	13	–1.64	–0.91	–11.85	3, 5
4	200702–200711	10	–1.18	–0.60	–6.01	10
5	200911–201012	14	–1.11	–0.60	–8.43	4, 5, 6
6	201208–201301	6	–0.43	–0.27	–1.36	10
7	201512–201612	13	–3.55	–2.15	–27.90	11, 12, 27
8	201706–201708	3	–0.75	–0.33	–1.00	29
9	201801–201805	5	–2.05	–1.42	–7.10	29
10	202003–202010	8	–0.79	–0.40	–1.81	11

anomalous increases in precipitation and decreases in surface temperature led to a flood disaster in the Amazon Basin in 2009. Figures 10(a)–10(f) show the TWS changes in the Amazon Basin over a two-month interval from September 2008 to July 2009. In September 2008, the TWS in the Amazon Basin was below average; by November, the TWS in the southwestern region started to increase; in January 2009, the TWS in the southern region was significantly higher than the normal level; in March, the flood had developed from the central region to the eastern region; in May, the flood peaked mainly in the central and eastern regions, and gradually subsided in July.

In October 2020, TWS changes reached a minimum of −15.98 cm in the Amazon Basin, with the GPCP showing continuous negative precipitation changes from June to November 2020, reaching a minimum of −9.72 cm in August. The CRU showed positive and continuous increases in surface temperature changes from August to October 2020, and reached a maximum of 0.85 °C in October. These results indicate that the decrease in TWS in the Amazon Basin in October 2020 was due to an abnormal decrease in precipitation and a continuous increase in surface

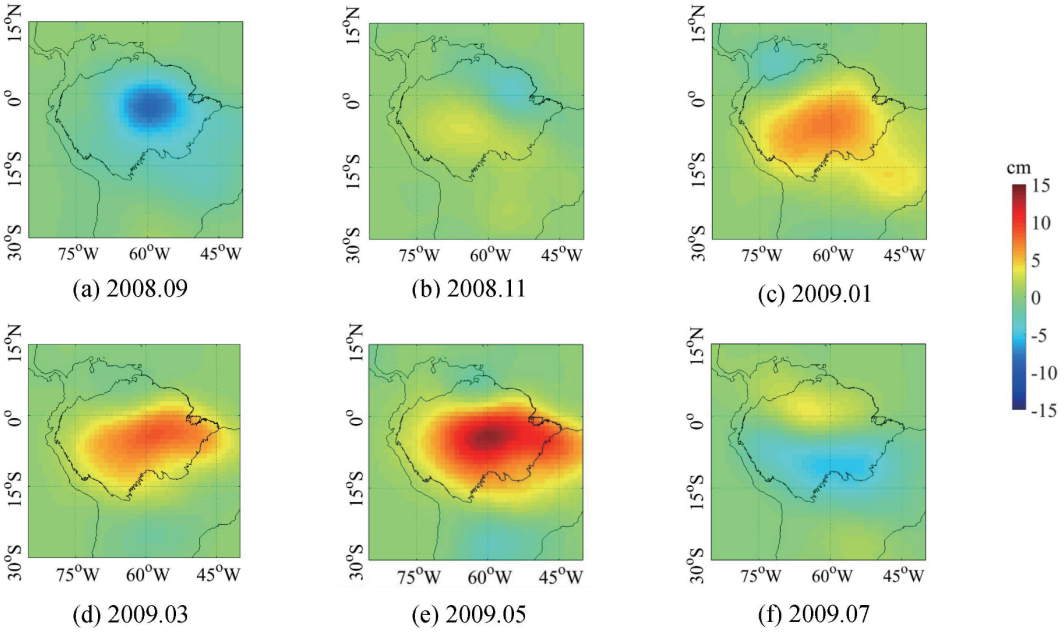

Fig. 10. (Color online) Evolution of monthly TWS changes in the Amazon Basin every two months during the period from September 2008 to July 2009.

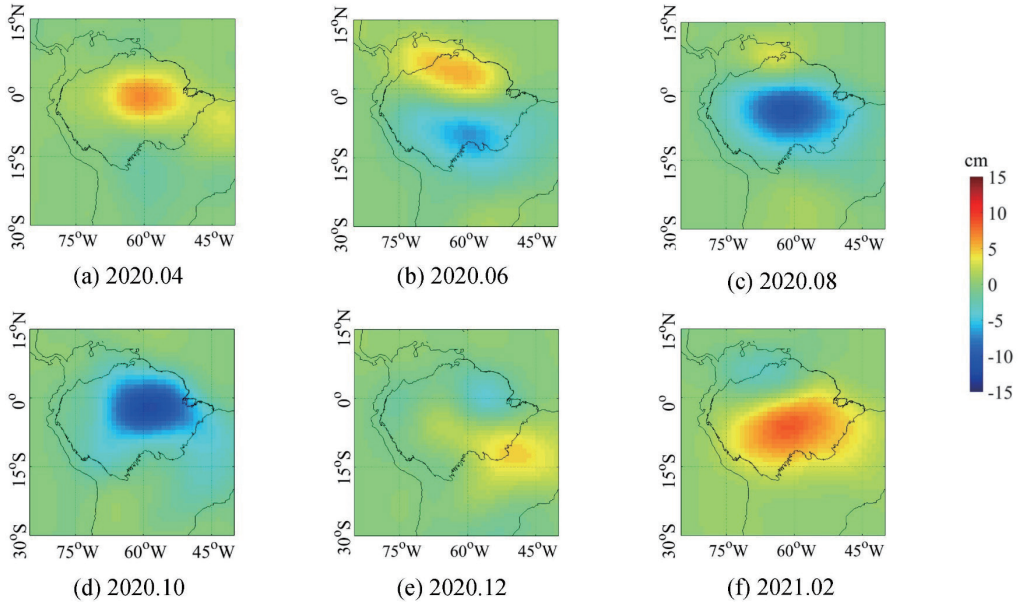

Fig. 11. (Color online) Evolution of monthly TWS changes in the Amazon Basin every two months during the period from April 2020 to February 2021.

temperature, which led to another drought disaster in the Amazon Basin. Figures 11(a)–11(f) show the TWS changes in the Amazon basin over two-month intervals from April 2020 to February 2021. In April 2020, the TWS in the Amazon Basin was slightly above average; in June, the TWS in the southern region started to decrease; in August, the TWS in the central

region was significantly below the normal level and the drought gradually shifted to the central region; in October, the drought mainly peaked in the northeastern region; in December, the drought gradually subsided; in February 2021, the TWS increased and the drought ended.

4. Conclusions

We combined GRACE, Swarm, and GRACE-FO satellite data to investigate the temporal and spatial variation characteristics of the TWS changes in the Amazon Basin over the last 20 years (April 2002 and December 2021). To verify the results, we compared the TWS changes with the GLDAS model. Moreover, we used GPCP precipitation data, CRU TS surface temperature data, and GLDAS evapotranspiration data to further analyze the factors affecting the TWS changes in the Amazon Basin. We also investigated the reasons for the 2009 flood and 2020 drought disasters in the Amazon Basin. The results were obtained as follows.

We assessed the combined filtering methods of Swenson filtering, Duan filtering, P4M6 filtering, and P4M15 filtering with Gaussian 300 km. The results that the combined P4M6 + Gaussian 300 km filtering provided are most similar to the GLDAS model.

The linear trend of TWS changes was an increase of approximately 0.23 ± 0.11 cm/a in the Amazon Basin, and the central and eastern regions had the highest increase rate, whereas the southeastern region showed a decreasing trend. In the last 20 years, maximum TWS variations occurred in April and minimum TWS variations occurred in October. In spring, the TWS in the Amazon Basin varies greatly from north to south, with an increase in the northern region and a decrease in the southern region. The summer is the season with the least amount of water stored. In winter, the TWS is the opposite to that in spring, with a decrease in the northern region and an increase in the southern region.

Precipitation and surface temperature are important factors affecting the TWS changes in the Amazon Basin. Conversely, the TWS changes have a limited relationship with evapotranspiration. The TWS changes observed by GRACE, Swarm, and GRACE-FO lagged behind the precipitation changes by approximately 64 days. The correlation coefficient between them was 0.57, which demonstrates a moderate correlation. However, precipitation changes (with a lag of two months) were significantly correlated with the TWS changes, with a correlation coefficient of 0.85, indicating that precipitation is an important factor affecting the TWS changes. In addition, the TWS changes were negatively correlated with surface temperature changes, with a correlation coefficient of −0.50, indicating that surface temperature affects the TWS changes.

The WSDI results detected 10 drought events in the Amazon Basin from April 2002 to December 2020, and the most recent occurred from March 2020 to October 2020. The decrease in TWS in October 2020 was related to an abnormal decrease in precipitation and a continuous increase in surface temperature, which resulted in a drought disaster in the Amazon Basin.

Acknowledgments

This work was supported by the National Key Research and Development Program (No. 2016YFB0501701) and the Capacity Development for Local College Project (No. 19050502100).

References

1 B. D. Tapley, S. Bettadpur, J. C. Ries, P. F. Thompson, and M. M. Watkins: Science **305** (2004) 503. https://doi.org/10.1126/science.1099192
2 J. Wahr, S. Swenson, V. Zlotnicki, and I. Velicogna: Geophys. Res. Lett. **31** (2004) 293. https://doi.org/10.1029/2004GL019779
3 J. L. Chen, C. R. Wilson, B. D. Tapley, Z. L. Yang, and G. Y. Niu: J. Geophys. Res.: Solid Earth **114** (2009) B05404. https://doi.org/10.1029/2008jb006056
4 J. L. Chen, C. R. Wilson, and B. D. Tapley: Water Resour. Res. **46** (2010) 439. https://doi.org/10.1029/2010wr009383
5 W. Feng, J.-M. Lemoine, M. Zhong, and H. Z. Xu: Chin. J. Geophys. **55** (2012) 814 (in Chinese). https://doi.org/10.6038/j.issn.0001-5733.2012.03.01
6 N. Nie, W. C. Zhang, H. D. Guo, and N. Ishwaran: J. Appl. Remote Sens. **9** (2015) 096023. https://doi.org/10.1117/1.JRS.9.096023
7 L. Pu, D. M. Fan, W. You, X. C. Yang, Z. M. Nigatu, and Z. S Jiang: Remote Sens. Lett. **13** (2022) 14. https://doi.org/10.1080/2150704X.2021.1981557
8 J. L. Chen, B. D. Tapley, M. Rodell, K.-W. Seo, C. Wilson, B. R. Scanlon, and Y. Pokhrel: Water Resour. Res. **56** (2020) e2020WR028032. https://doi.org/10.1029/2020WR028032
9 C. Lück, J. Kusche, R. Rietbroek, and A. Löcher: Solid Earth **9** (2018) 323. https://doi.org/10.5194/se-9-323-2018
10 L. L. Cui, Z. Song, Z. C. Luo, B. Zhong, X. L. Wang, and Z. B. Zou: Water **12** (2020) 3128. https://doi.org/10.3390/w12113128
11 J. Xiang, Z. T. Wang, and K. J. Tian: Sci. Surv. Mapp. **47** (2022) 116 (in Chinese). https://doi.org/10.16251/j.cnki.1009-2307.2022.03.016
12 F. P. Li, Z. T. Wang, N. F. Chao, J. D. Feng, B. B. Zhang, K. J. Tian, and Y. K. Han: Geomatics Inf. Sci. Wuhan Univ. **45** (2020) 595 (in Chinese). https://doi.org/10.13203/j.whugis20180273
13 B. Braga, P. Varella, and H. Goncalves: Int. J. Water Resour. Dev. **27** (2011) 477. https://doi.org/10.1080/07900627.2011.595382
14 E. M. Latrubesse, E. Y. Arima, T. Dunne, E. Park, V. R. Baker, F. M. D'Horta, C. Wight, F. Wittmann, J. Zuanon, P. A. Baker, C. C. Ribas, R. B. Norgaard, N. Filizola, A. Ansar, B. Flyvbjerg, and J. C. Stevaux: Nature **546** (2017) 363. https://doi.org/nature22333
15 S. Bettadpur: UTCSR Level-2 Gravity Field Product User Handbook (The Universtiy of Texasat at Austin, Austin, 2007) GRACE p. 327.
16 D. E. Teixeira, D. Arnold, A. Bezděk, C. Dahle, E. Doornbos, J. V. D. Ijssel, A. Jäggi , T. Mayer Gürr, J. Sebera, P. Visser, and N. Zehentner: Earth Planets Space **68** (2016) 1. https://doi.org/10.1186/s40623-016-0499-9
17 J. Wahr, M. Molenaar, and F. Bryan: J. Geophys. Res.: Solid Earth **103** (1998) 30205. https://doi.org/10.1029/98jb02844
18 S. Yang, W Zheng, W. J. Yin, and J. Liu: Chin. J. Geophys. **64** (2021) 3068 (in Chinese). https://doi.org/10.6038/cjg2021O0431
19 S. Swenson, D. Chambers, and J. Wahr: J. Geophys. Res.: Solid Earth **113** (2008) B08410. https://doi.org/10.1029/2007jb005338
20 M. K. Cheng and B. D. Tapley: J. Geophys. Res.: Solid Earth **109** (2004) B09402. https://doi.org/10.1029/2004jb003028
21 A. Geruo, J. Wahr, and S. J. Zhong: Geophys. J. Int. **192** (2013) 557. https://doi.org/10.1093/gji/ggs030
22 S. Swenson and J. Wahr: Geophys. Res. Lett. **33** (2006) L08402. https://doi.org/10.1029/2005GL025285
23 X. J. Duan, J. Y. Guo, C. K. Shum, and W. V. D. Wal: J. Geod. **83** (2009) 1095. https://doi.org/10.1007/s00190-009-0327-0
24 J. L. Chen, C. R. Wilson, D. Blankenship, and B. D. Tapley: Nat. Geosci. **2** (2009) 859. https://doi.org/10.1038/ngeo694
25 D. Chambers and J. A. Bonin: Ocean Sci. **8** (2012) 859. https://doi.org/10.5194/os-8-859-2012
26 T. H. Syed, J. S. Famiglietti, M. Rodell, J. L. Chen, and C. R. Wilson: Water Resour. Res. **44** (2008) W02433. https://doi.org/10.1029/2006WR005779
27 J. C. Jiménez-Muñoz, C. Mattar, J. Barichivich, A. Santamaría-Artigas, K.Takahashi, Y. Malh, J. Sobrino, and G. V. D. Schrier: Sci. Rep. **6** (2016) 1. https://doi.org/10.1038/srep33130
28 R. D. Goncalves, R. Stollberg, H. Weiss, and H. K. Chang: Sci. Total Environ. **705** (2020) 135845. https://doi.org/10.1016/j.scitotenv.2019.135845
29 L. L. Cui, M. Q. Yin, Z. K. Huang, C. L. Yao, X. L. Wang, and X. Lin: Remote Sens. **14** (2022) 2887. https://doi.org/10.3390/rs14122887

About the Authors

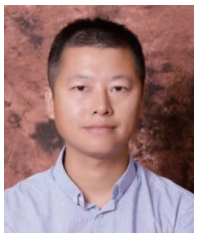

Kuifeng Luan received his B.S. degree from Liaoning Technical University, China, in 2004 and his Ph.D. degree from Tongji University, China, in 2017. From 2015 to 2019, he was a lecturer at Shanghai Ocean University, China. Since 2019, he has been an associate professor at Shanghai Ocean University, China. His research interests are in ocean observation based on satellite and LiDAR data quality control. (kfluan@shou.edu.cn)

Jiancong Hu received his B.S. degree from Guangdong University of Finance & Economics, China, in 2021. He is currently an M.S. student of the College of Marine Sciences at Shanghai Ocean University, China. His research interest is in satellite gravimetry. (m210200630@st.shou.edu.cn)

Guiping Feng received his B.S. degree from Wuhan University, China, in 2010 and his Ph.D. degree in geodesy from the University of Chinese Academy of Sciences, China, in 2014. Since 2014, he has been a lecturer at Shanghai Ocean University, China. His research interests are in ocean circulation, satellite gravimetry, and satellite oceanography. (gpfeng@shou.edu.cn)

Zhenge Qiu received his B.S. degree from Wuhan University, China, in 1987 and his M.S. and Ph.D. degrees from the Information Engineering University, China, in 1993 and 2001, respectively. Since 2012, he has been a professor at Shanghai Ocean University, China. His research interest is in marine mapping. (zgqiu@shou.edu.cn)

Kunning Zhang received his B.S. degree from Chuzhou University, China, in 2019 and his M.S. degree from Shanghai Ocean University, China, in 2022. His research interests are in ocean remote sensing and LiDAR data quality control. (m190200504@st.shou.edu.cn)

Weidong Zhu received his B.S. degree from Henan Polytechnic University, China, in 2003, his M.S. degree from Jiangxi University of Science and Technology, China, in 2008, and his Ph.D. degree from Tongji University, China, in 2011. Since 2011, he has been a lecturer at Shanghai Ocean University, China. His research interests are in hyperspectral image processing, coastal remote sensing, and GNSS precise point positioning. (wdzhu@shou.edu.cn)

Jie Wang received her B.S. and M.S. degrees from Shandong University of Science and Technology, China, in 2003 and 2006, respectively. She received her Ph.D. degree from the University of Chinese Academy of Sciences, China, in 2008. Since 2013, she has been an associate professor at Shanghai Ocean University, China. Her research interest is in ocean remote sensing. (wangjie@shou.edu.cn)

Zhenhua Wang received her B.S. degree from Yantai Normal University, China, in 2010, her M.S. degree from the Chinese Academy of Sciences, China, in 2007, and her Ph.D. degree from Tongji University, China, in 2010. From 2010 to 2015, she was a lecturer at Shanghai Ocean University, China. Since 2015, she has been an associate professor at Shanghai Ocean University, China. Her research interests are in spatial data analysis, data quality control, and deep learning. (zh-wang@shou.edu.cn)